







Article

A Long-Range Internet of Things-Based Advanced Vehicle Pollution Monitoring System with Node Authentication and Blockchain

Arti Rana ¹, Arvind Singh Rawat ², Ashraf Affi ³, Rajesh Singh ^{1,4}, Mamoon Rashid ^{5,*}, Anita Gehlot ^{1,4}, Shaik Vaseem Akram ^{1,6} and Sultan S. Alshamrani ⁷

- ¹ Uttaranchal Institute of Technology, Uttaranchal University, Dehradun 248007, India; artirana@uttaranchaluniversity.ac.in (A.R.); rajeshsingh@uttaranchaluniversity.ac.in (R.S.); anita.ri@uttaranchaluniversity.ac.in (A.G.); vaseemakram5491@gmail.com (S.V.A.)
- ² Collaborative Microelectronic Design Excellence Centre (CEDEC), Engineering Campus, Universiti Sains Malaysia, George Town 11900, Malaysia; arvindsrawat@ieee.org
- ³ Department of Computer Engineering, College of Computers and Information Technology, Taif University, P.O. Box 11099, Taif 21944, Saudi Arabia; a.affi@tu.edu.sa
- ⁴ Department of Project Management, Universidad Internacional Iberoamericana, Campeche C.P. 24560, Mexico
- ⁵ Department of Computer Engineering, Faculty of Science and Technology, Vishwakarma University, Pune 411048, India
- ⁶ Law College of Dehradun, Uttaranchal University, Dehradun 248007, India
- ⁷ Department of Information Technology, College of Computers and Information Technology, Taif University, P.O. Box 11099, Taif 21944, Saudi Arabia; susamash@tu.edu.sa
- * Correspondence: mamoon.rashid@vupune.ac.in; Tel.: +91-7814346505



Citation: Rana, A.; Rawat, A.S.; Affi, A.; Singh, R.; Rashid, M.; Gehlot, A.; Akram, S.V.; Alshamrani, S.S. A Long-Range Internet of Things-Based Advanced Vehicle Pollution Monitoring System with Node Authentication and Blockchain. *Appl. Sci.* **2022**, *12*, 7547. <https://doi.org/10.3390/app12157547>

Academic Editors: Antoaneta Ene and Claudia Stihl

Received: 5 July 2022

Accepted: 26 July 2022

Published: 27 July 2022

Publisher's Note: MDPI stays neutral with regard to jurisdictional claims in published maps and institutional affiliations.



Copyright: © 2022 by the authors. Licensee MDPI, Basel, Switzerland. This article is an open access article distributed under the terms and conditions of the Creative Commons Attribution (CC BY) license (<https://creativecommons.org/licenses/by/4.0/>).

Abstract: According to United Nations (UN) 2030 agenda, the pollution detection system needs to be improved for the establishment of fresh air to obtain healthy life of living things. There are many reasons for the pollution and one of the reasons for pollution is from the emissions of the vehicles. Currently digital technologies such as the Internet of Things and Long-Range are showing significant impact on establishment of smart infrastructure for achieving the sustainability. Based on this motivation, this study implemented a sensor node and gateway-based Internet of Things architecture to monitor the air quality index value from any location through Long-Range communication, and Internet connectivity. To realize the proposed system, a customization of hardware is carried out and implemented the customized hardware i.e., sensor node and gateway in real-time. The sensor node is powered with node mapping to minimize the data redundancy. In this study, the evaluation metrics such as bit rate, receiver sensitivity, and time on air are evaluated by spreading factor (SF), code rate (CR), bandwidth, number of packets, payload size, preamble, and noise figure. The real-time sensor values are logged on the cloud server through sensor node and gateway. The sensor values recorded in the cloud server is compared with optimal values and concluded that the PM₁₀, PM_{2.5} are high in the air and remaining values of NO₂, O₃, CO are optimal in the air. Along with this an architecture is proposed for interfacing the hardware with blockchain network through cloud server and API for node authentication.

Keywords: cloud server; Long-Range; Internet of Things; pollutant emissions; sensors; vehicular pollution

1. Introduction

According to the United Nations (UN), sustainable development goals (SDG) are also focused on minimizing environmental pollution by 2030 for providing clean air to the people. The environment constitutes everything around including air, water, and the ecosystem which supports life. Not only the environment but an environment that is clean in quality is required for the prosperous and healthy survival of humans [1]. The quality of the air is dependent on the optimal range of the pollutants that release from the different

activities such as industries, vehicles, etc. Air pollution caused by automobiles is one of the hazardous challenges that continues to cause harm to the environment [2]. Vehicular pollution may result either from evaporative emissions, refueling losses, or exhaust emissions. The fumes resulting from exhaust emissions are one of the key constituents. The composition is a mixture of gasses such as carbon dioxide, carbon monoxide, and oxides of nitrogen [3,4]. The government of any country has taken many actions to take the situation in control; however, there are limitations in the scenario of manual monitoring [5].

With the advancement and evolution of technologies such as the Internet of Things, Long-Range communication has encouraged implementing the automation and real-time monitoring system with wireless sensors and blockchain. The sensory data obtained from the sensors with geo-location assist to supervise the pollutants level of the particular area on the digital platform (cloud server). With the motivation from these facts, this study aims to implement an Internet of Things and Long-Range-based cloud server for real monitoring of vehicle pollutants levels. To achieve the proposed system, hardware customization is performed and the customized hardware, i.e., sensor node and gateway, is implemented in real-time. To reduce data redundancy, the sensor node is powered via node mapping. The sensor node and gateway log the real-time sensor values on the cloud server. The sensor results stored in the cloud server are compared to optimal values, and it is concluded that the PM₁₀ and PM_{2.5} levels are high in the air, while the remaining NO₂, O₃, and CO levels are optimal. In addition, an architecture for integrating the hardware with the blockchain network via cloud server and API for node authentication is proposed.

The main contribution of this study is as follows:

- Long range communication and Internet of Things-based architecture is proposed for real-time monitoring of vehicular pollution.
- Customized sensor node and gateway are developed for the real-time implementation.
- The evaluation metrics such as bit rate, receiver sensitivity, and time on air are evaluated by spreading factor (SF), code rate (CR), bandwidth, number of packets, payload size, preamble, and noise figure.
- The sensor node and gateway are deployed in the real-time environment and logged the sensor value on the cloud server.
- An architecture is proposed for interfacing the hardware with blockchain network through cloud server and API.

The rest of this paper is arranged as follows. Section 2 describes the overview of air pollution and associated problems with vehicular pollution. Section 3 discusses the literature review in detail. Section 4 discusses the methodology used to achieve the proposed objective. Section 5 discusses the hardware implementation. Section 6 illustrates the evaluation metrics of Long-Range network. Section 7 discusses the results and finally, Section 8 concludes the proposed work.

2. Overview of Air Pollution

Air pollution is one of the major environmental issues which has been ignored but should be dealt with carefully so that there is a permanent solution for it. It has not only affected the humans but also the economy of a country. According to [6], the pollutant emissions from diesel engines comprise hydrocarbons (HC), carbon monoxide (CO), nitrogen oxides (NO_x), and particulate matter (PM) which are the major causes of air pollution. Particle pollution, ground-level ozone, CO, sulfur oxides, NO_x, and lead are the six main air pollutants that the World Health Organization (WHO) measures. Groundwater, soil, and air are just a few of the elements of the ecosystem that can be severely harmed by air pollution. Studies concentrating on either short-term (acute) or long-term (chronic) PM exposure have demonstrated a link between PM and unfavorable health consequences [7]. These particles have been associated with major health issues i.e., short-term effects (headache, coughing, pneumonia, breathing, bronchitis, skin irritation) and long-term effects (affecting the central nervous system, impacts on the liver and reproductive system, cardiovascular disease, and respiratory disease) [8].

There are many reasons which have contributed to the rise of air pollution such as urbanization, vehicular emissions, or industrial emissions and a conclusion can be made that the careless utilization of resources of nature is the main source of air pollution. Readings refer to particulate substances that are having a diameter of fewer than 2.5 μm is defined as $\text{PM}_{2.5}$. Figure 1 shows the top twenty cities of the world that are most polluted which are measured based on $\text{PM}_{2.5}$. The automobile is one of the sectors having a prominent role in the development of any country and its economy. But it is also one of the reasons that have polluted the air. Taking reference from the past, with the increase in the number of vehicles, there is a tremendous decrease in the quality of air. Depending on the quality of the fuel they consume and the efficiency of their engines, automobiles generate a variety of pollutants. The discharge of pollutants from automobiles also includes fugitive fuel emissions, the source, and level depending on the vehicle type, maintenance, and other factors.

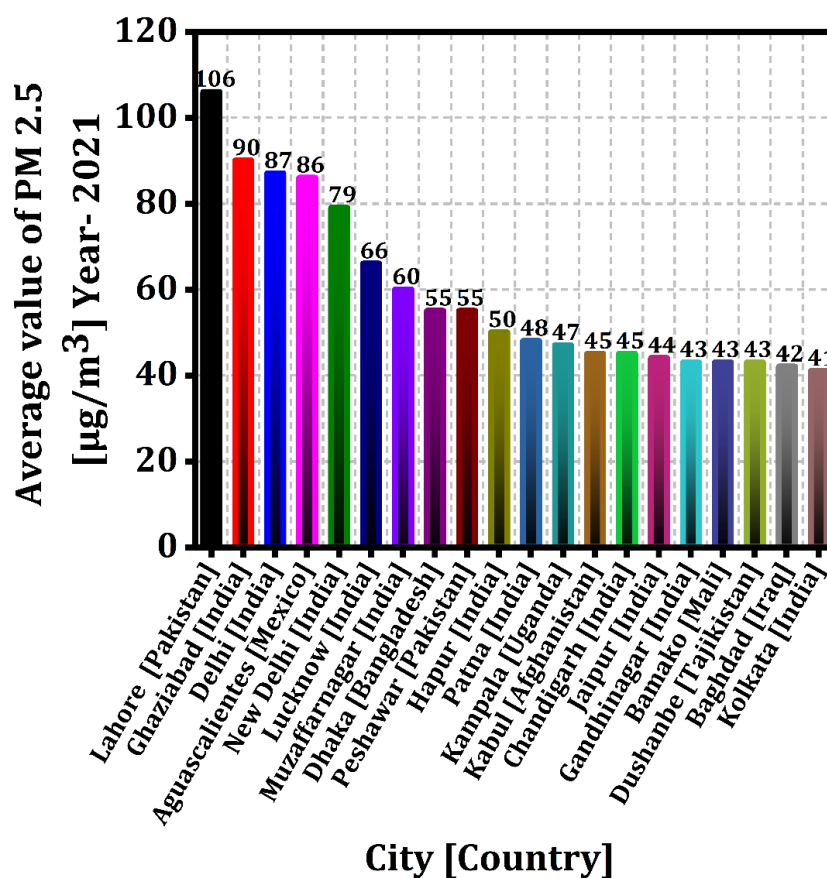


Figure 1. Twenty most polluted cities across the globe (2021 Rankings). Source: <https://smartairfilters.com/en/blog/25-most-polluted-cities-world-2021-rankings/>. accessed on 12 June 2022.

2.1. Analysis

Out of the 20 most polluted cities in the world, eleven are in India, while 2 are in Pakistan. The government has taken many actions to control the situation but looking at Figure 1 which represents the cities that are most polluted worldwide in 2021, an observation can be made that all steps that have been taken for solving the problem of air pollution are not sufficient. Therefore, more and more attempts to controlling air pollution should be made, providing a solution that can improve the condition so that the healthy life of the organisms can be maintained.

2.2. Vehicular Pollutants

The sources (i.e., mobile sources include transportation vehicles, trucks, plains, and trains, and stationary sources include oil refineries, power plants, factories, and industrial

facilities and area sources include cities, wood-burning fireplaces, agricultural areas, and natural sources include volcanoes, wind-blown dust, and wildfires [9]) of global pollutant emissions vary, with transportation being one among them. Even though transportation (vehicles) is not the most significant source of pollution emissions on a worldwide scale, it is a big problem in densely populated metropolitan areas. Large cities suffer from heavy traffic, which results in high levels of pollutant emissions, which have a direct and indirect influence on human health. Pollutant emissions from internal combustion engines could be divided into two categories (Figure 2).

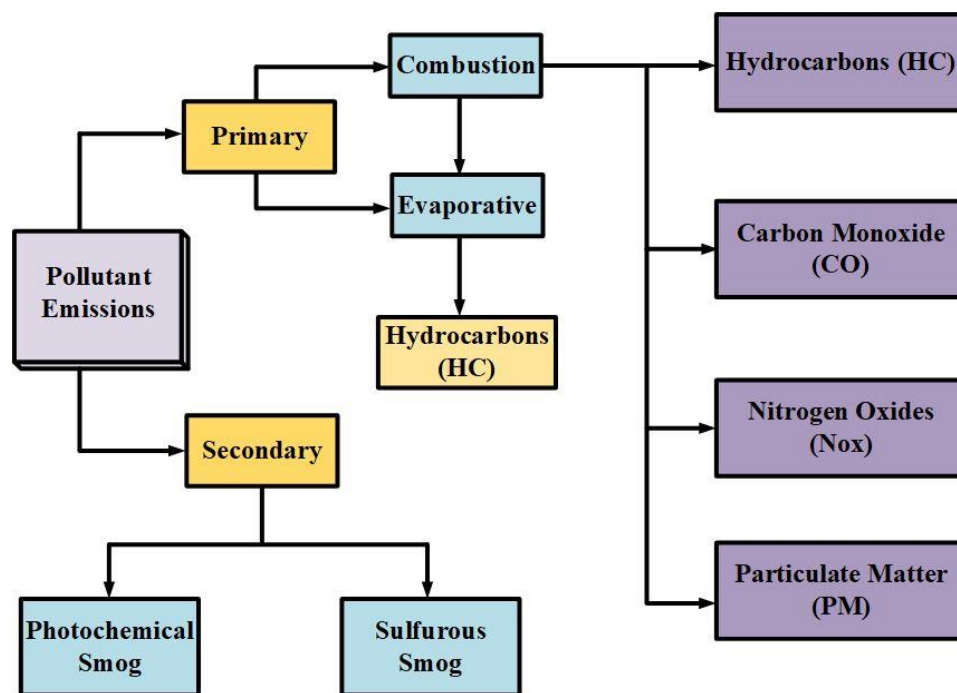


Figure 2. Types of pollutant emissions from vehicles with internal combustion engines.

Every vehicle emits or releases pollutants that become the reason for leveraging the level of air pollution. This emission depends on the nature of the fuel that is fed to the vehicle. Various emissions such as CO, HC, and oxides of nitrogen are the pollutants that are released by vehicles which form the area of concern. Table 1 shows the summarized effects of these pollutants on humans, environment, and climate. This means that the pollutants affect not only the environment but also living organisms directly or indirectly in one or some other way [10,11].

Table 1. Effects from pollutants on humans, environment, and climate.

Pollutants	Health Effect		Environmental Effects			Climate Change	
	Direct	Indirect	Acid Rains	Eutrophication	Visibility	Direct	Indirect
CO	Yes	No	Yes	No	No	No	Yes
HC	Yes	Yes	Yes	Yes	No	No	Yes
NOx	Yes	Yes	Yes	Yes	Yes	Yes	No
PM	Yes	No	Yes	No	Yes	Yes	No
SOx	Yes	No	Yes	No	Yes	No	Yes

3. Literature Review

The various components contaminate the environment, some of them are artificial and others are due to natural factors. Moreover, the role of environmental monitoring becomes crucial in addressing the difficulties in order to maintaining the environment for

a healthy society and world [12]. The entire world is working together to preserve the environment for sustainable agriculture, development, and a healthy society. The main goal of smart environment monitoring is to deal with the challenges posed by harmful emissions through smart monitoring, ensuring that all key factors of growth, including societal health, are well controlled. Environment monitoring strategies are used for a variety of objectives, including air pollution prevention and control [13], water quality control, and monitoring [14]. The authors introduced the name VehNode, a wireless sensor network (WSN)-based vehicular pollution monitoring platform able to measure various types of pollution levels included in emissions generated by an automobile and automatically report the status to the appropriate agencies as necessary. Following the web of things concept, their work guaranteed the presence of a wireless sensor network platform for vehicle pollution management, concentrating on simple access to real-time data over the web [15].

In [16], the author suggested a model that is capable of simple routing as well as emergencies and traffic rule breaches. They employed infrared sensors (IR) to monitor the number of vehicles and aid in the detection of emergency vehicles, image sensors to detect traffic offenses, and microphone sensors to determine the frequency of emergency vehicles using an advanced algorithm. Machine learning and image processing techniques were used in their research. [17] suggested the design and deployment of a variety of remotely linked sensor modules for monitoring indoor air quality factors and capturing the data in real-time. This is accomplished through the use of infrared-based sensor technology that detects CO₂, temperature, and humidity, low-power networking technologies, and geographical prediction using geostatistical approaches. The infrastructure is comprised of an MBED LPC 1768 control board that obtains data from sensor nodes and wirelessly delivers it to a central unit through a ZigBee module, where it is evaluated and preserved. On live data, geographical forecasting is also conducted in real-time. Air pollution is extremely bad in metropolitan areas. Because of car emissions and hazardous gas emissions from industry, air quality in metropolitan areas deteriorates. WSN and low-cost ambient sensors were employed for real-time monitoring of air quality in metropolitan areas [18]. The appropriate design framework of an intelligent transportation system based on Internet of Things technology was proposed in [19].

The findings of the experiments reveal that the intelligent transportation system can accurately and efficiently implement the information exchange between the vehicle and the control center as well as anticipate road conditions. Simultaneously, the intelligent transportation system may increase vehicle speed on the road, make more efficient use of resources, decrease economic losses during vehicle operation, and reduce air pollution from gasoline emissions. In [20], the authors presented a smart sensor system based on the green Internet of Things that employs a wireless sensor in association with a Long-Range module to measure vehicle emissions. For communication between automobiles and road side units (RSU), gas sensors coupled to a node MCU equipped with Long-Range are employed. If the emission rate reaches the threshold limit from the given specifications set by pollution under control (PUC) authorities, the vehicle information and owner details will be captured and sent to the nearest traffic signal post connected with the amazon web service (AWS) Internet of Things cloud and relational database service (RDS), and the vehicle owner will be notified. In [21], the author implemented a UAV network based on the Internet of Things and a cloud server for the smart city for tracking the air quality. The gas that causes the most air pollution is NO₂, volatile organic compounds (VOC), CO, SO₂, ozone, dioxins, furans, etc.

In [22], the authors presented an Internet of Things-based low power wide area (LPWA) air quality monitoring system (AQMS). It is divided into three layers: the sensor layer, the network layer, and the application layer. The sensing layer comprises the sensors that are positioned throughout vast geographical regions. The sensor nodes collect data and send it to the network layer. The LPWA network layer ensures pervasive communication between sensor nodes and access points. Implementing a directly sequenced spread spectrum improves the sensitivity of the receivers. Open source software-defined radio was used to

create an access point. The network data are processed at the application layer, which is separated into two components. The authors of [23] presented a raspberry pi-based Internet of Things-enabled AQMS. The method consists of sensor motes that are coupled to raspberry pi with computational capability and a local SQL database. The data acquired from sensors are sent from the processing power to the thing speak cloud services via the wi-fi module, which is connected to the network router. MATLAB code is used to examine data saved in cloud services. The findings of data analytics are sent to user devices as alerts. [24] defined the usage of a blockchain to store data on air pollution. PM₁₀ and PM_{2.5}, VOC, and NO₂ concentrations are all measured using an Internet of Things-based sensor network.

Weather parameters and vehicular traffic statistics are also included in the data collection. Their project envisions data being recovered from a standard not structured query language (NoSQL) database and structured according to specified requirements being uploaded to the ethereum blockchain on a daily basis, with the option to manually select the time period of interest. The author proposed a three-phase air quality surveillance system in [25]. Gas sensors, an arduino integrated development environment (IDE), and a wi-fi module was used to create an Internet of Things kit. To monitor air pollution, this equipment may be practically deployed in several regions. The gas sensors collect information from the air and send it to the arduino IDE. The wi-fi device in the arduino IDE sends the data to the cloud. They created the Internet of Things- mobair android app, which allows users to get essential air quality data from the cloud. When a user travels to a location, the pollution level throughout the whole route is anticipated, and if the pollution level is too high, a warning is presented. As an alternative to permanent air quality monitoring stations presented in [26], a remote sensing system is meant to monitor air quality in chosen zones, with a particular focus on larger cities and densely populated industrial zones. The Internet of Things has been shown to benefit us in all aspects of our lives. The Internet of Things smart sensor system empowers smart machine sensing, data gathering, pre-processing, interaction, and communication. As a result, improving the dependability of smart sensor systems to aid in the collection of data with more real-time and meaningful information is critical in Internet of Things [27].

IB-AQMS blockchain nodes are usually dedicated servers hosted by cloud sources. The blockchain nodes are connected in a Peer-2-Peer distributed network, with nodes belonging to different organizations. Each organization must have numerous peer nodes where the blocks' copies are stored. Each block hashes the preceding blocks' hashed values, as well as transaction data and a timestamp. The implementation of blockchain for Internet of Things cloud applications is one of the most prominent services we have chosen in this study. The smart contract is another key mechanism for making digital transactions on the blockchain network. In general, a smart contract is a digital transaction contract with agreement provisions specified in computer languages [28]. Ref. [29] introduced the idea of the smart contract in the 1990s. In a conventional contract, two parties sign a paper agreement with numerous conditions, and these may be simply manipulated. But in the case of a smart contract, the agreement is formed in digital form, with the terms stated in a computer language. When specified conditions mentioned in the smart contract are fulfilled, the smart contract implements the agreement clauses. Furthermore, the smart contract enables us to use digital signatures in the peer-to-peer network to perform communications among two different nodes in a legal and encrypted manner.

From all the above reviews, it has been observed that all the research has been done and limited only to monitoring air pollution. While proposed work introduces Long-Range-Internet of Things-based vehicular pollution monitoring system using node authentication and blockchain. The hardware integration with blockchain network for vehicle air pollution need to be explored.

4. Proposed Work

In this section, we discuss about the proposed architecture for vehicle pollution monitoring using Internet of Things and Long-Range communication. In addition to this, a blockchain-based architecture is also proposed for interfacing the hardware devices with blockchain network.

4.1. Internet of Things and Long-Range Based Architecture

The proposed work relates to the field of a vehicular pollution detection system using more specifically an Internet of Things-based control system. Every vehicle emits or releases pollutants that become the reason for leveraging the level of air pollution. This emission depends on the quality or nature of the fuel that is fed to the vehicle. The model of the proposed system consists of various phases that help to study the working. The working of the proposed starts by setting up the devices in the vehicle. After the device is set up with the availability of Wi-Fi, thresholds for different emissions are set up in accordance with the government rules. When the vehicle starts, the phase of sensing of emission, i.e., data sensing starts. The data are continuously transferred to the cloud server in regular intervals and with this, the phase of monitoring starts. After monitoring, data analysis is carried on which helps to determine the actions. Figure 3 shows the general architecture of the proposed system where “N” numbers of vehicles related to the Long-Range Gateway which is a transceiver module and Wi-Fi modem employed for communicating the Internet packets to the cloud server on the Internet. Data are accessed from a cloud server via a web app or mobile application. Referring to Figure 4, shows the vehicular unit (1 to N), sensor array, signal conditioning device, controller unit which consists of an analog-to-digital converter chip and parts per million (PPM) chip, and Long-Range RF module, whereas Figure 5 represents the Long-Range gateway node of the current architecture for relaying transmission lines to the monitoring authority. The gateway converts RF transmissions into IP packets so that information can be communicated across the Internet protocol.

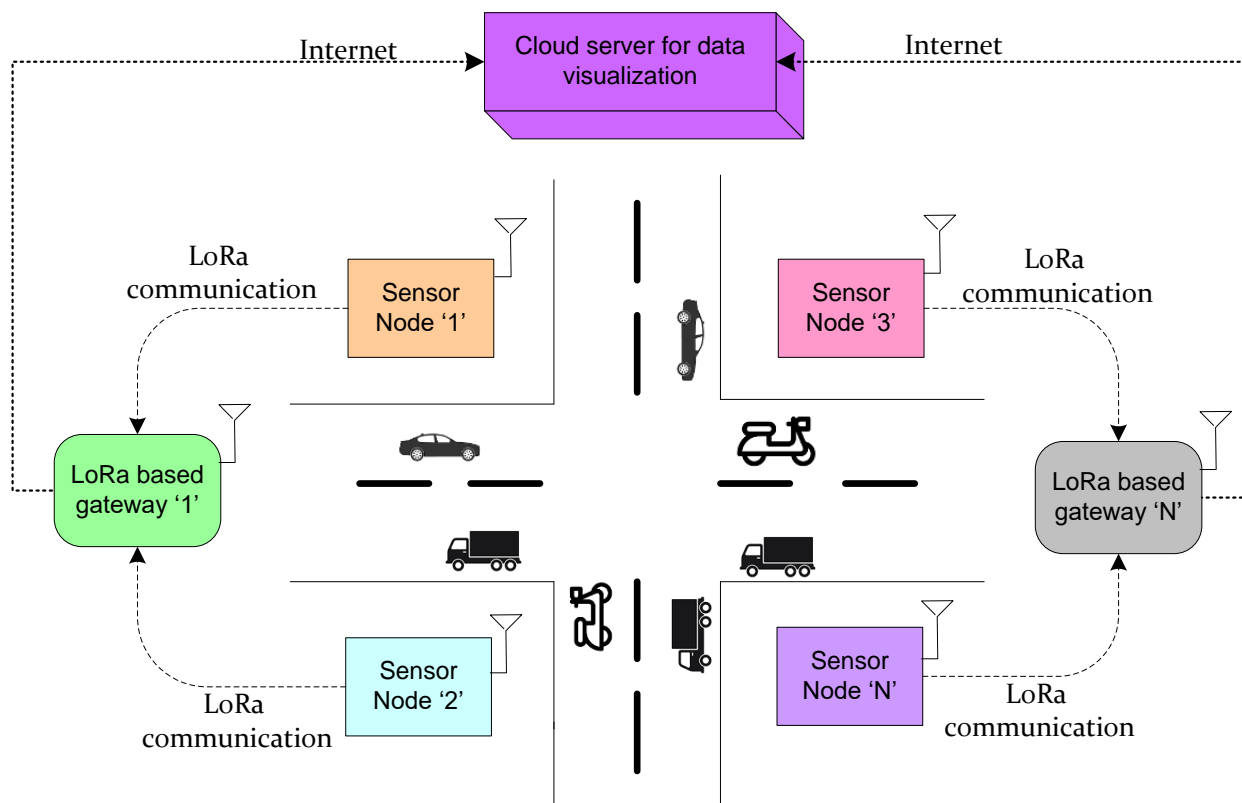


Figure 3. General architecture of the proposed system.

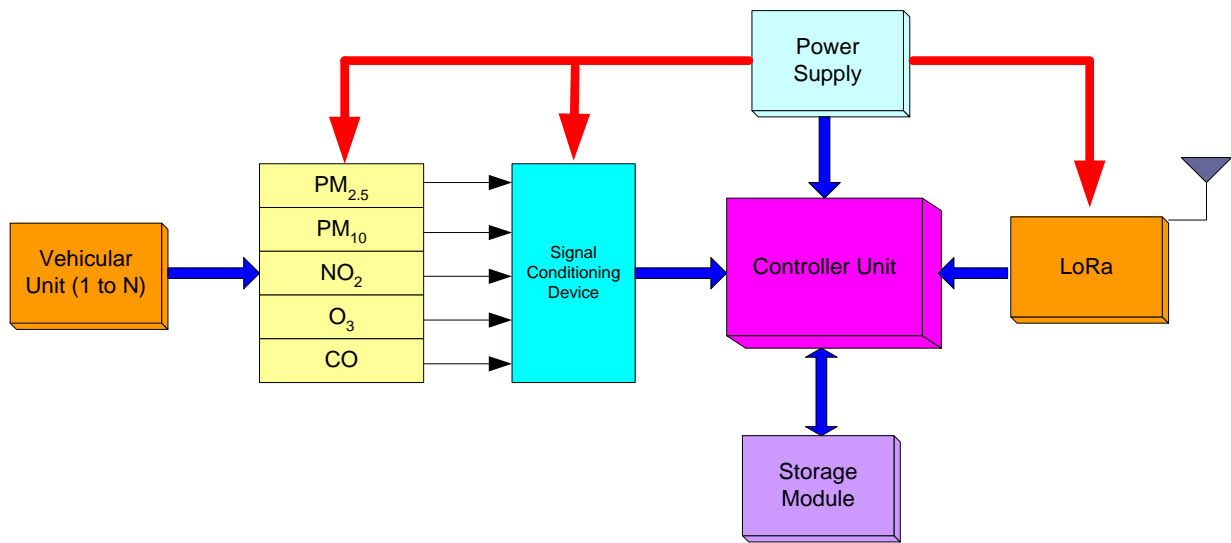


Figure 4. Sensor units.

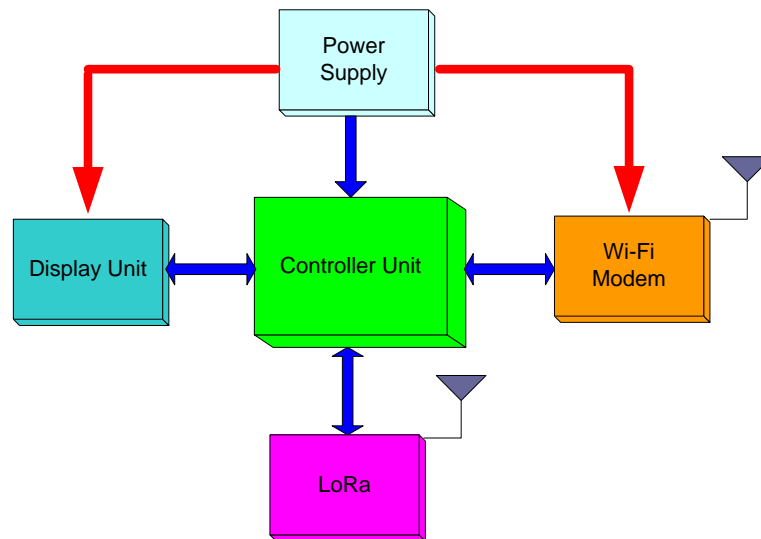


Figure 5. Range Gateway.

4.2. Phases of the Proposed System

The model of the proposed system consists of various phases that help to study the working structure. Figure 6 shows the phases involved in the proposed system.

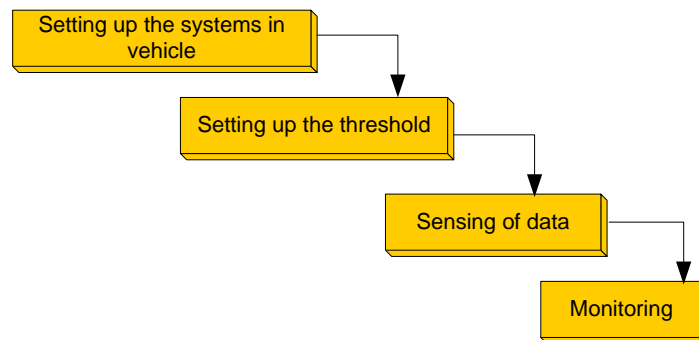


Figure 6. Model of the proposed system.

4.2.1. Setting up the System in the Vehicle

The information about the pollutants or the nature of pollutants from the vehicles is known by using PM₁₀, PM_{2.5}, NO₂, O₃, and CO sensors. Therefore, the first phase involves a connection between the hardware devices that would be attached to the vehicle and ensure the working of software tools that are needed. The Wi-Fi connection needs to be active, i.e., there should be Internet availability. The phase involves a connection set up in such a way that it would not hinder the working of a vehicle but would also be able to continue in its process effectively. Once the setup is done then there is no need for interaction from humans.

4.2.2. Setting up the Threshold

In this phase, the thresholds setting is done that depends on the standards set by the government. The threshold of a particular pollutant reflects the limit up to which the concentration of the pollutant is safe to emit to the environment i.e., the maximum limit to which no actions would be taken. If a vehicle crosses this limit, then there would be a problem. The thresholds set may be different or maybe the same depending upon the type of vehicle.

4.2.3. Sensing of Data

Up to this phase, the system is attached to the vehicle. The vehicle can go anywhere and then this phase starts. In this phase, as the vehicle carry out different actions, the sensors collect data regarding the levels of the emission of the different pollutants. Data are converted to PPM standard but, these data are not sent directly to the server because a vehicle does not need to produce emissions above the threshold always, keeping this fact in mind, a solution is proposed in which the average of the data from a single day for each pollutant would be sent for further procedure.

4.2.4. Monitoring

After the sensing part of the system, the desired output has reached the cloud server and at this repository, the monitoring could be done in the public domain. In the monitoring phase, the data are checked for a vehicle and if the data of a vehicle are continuously crossing the threshold for a specific period, then this indicates that the vehicle needs servicing and the alert for the same would be sent to the owner and the traffic police department.

4.3. Blockchain-Based Architecture for Hardware Interfacing

Figure 7 depicts the information flow in the smart contract during transactions, which determines the production of blocks and database updates. After the consensus agreement algorithm, the transaction to execute the rules of smart contracts for verifying data must check at least 50% of the information inputs and transactions to update the blockchain network's database [30]. The network's consensus nodes verify and confirm the transactions. After the verification and validation of transactions, the "blocks" are formed, added, and transmitted to comparable blocks in the network.

Figure 8 illustrates the proposed architecture for hardware interfacing with blockchain network. A data source is a full system that includes Internet of Things devices, edge nodes, fog nodes, gateways, and cloud servers. The data sent to the cloud server from Internet of Things devices are linked to the blockchain via an API. Entry of the new data is considered as new transactions in this case, and a new block is formed. This transaction is sent to different nodes for mining, where all the nodes are unique entities. As soon as a transaction is made, the miners' obligation is invoked. For validation, miners use the "Proof of Work" algorithm used by the nodes. If the transaction is valid, it is added to the new block's chain. Furthermore, the fog node validates the number of proofs performed by nodes, as well as numerous chains resolved by consensus, while verifying nodes. The transaction is added to the new block and recorded into the database if the nodes are authentic.

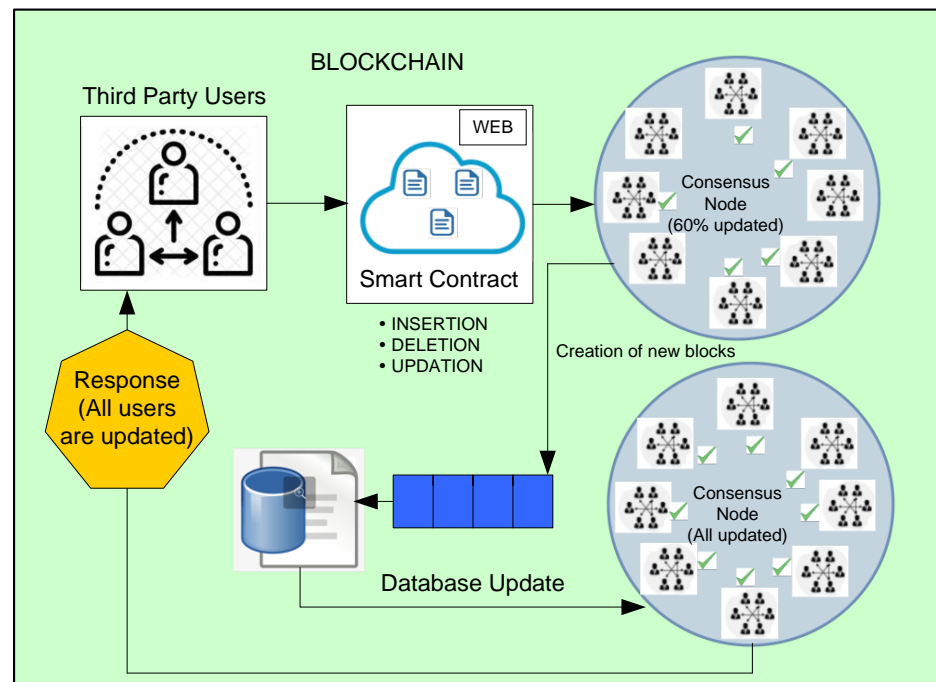


Figure 7. Process of transaction of information along with smart contracts.

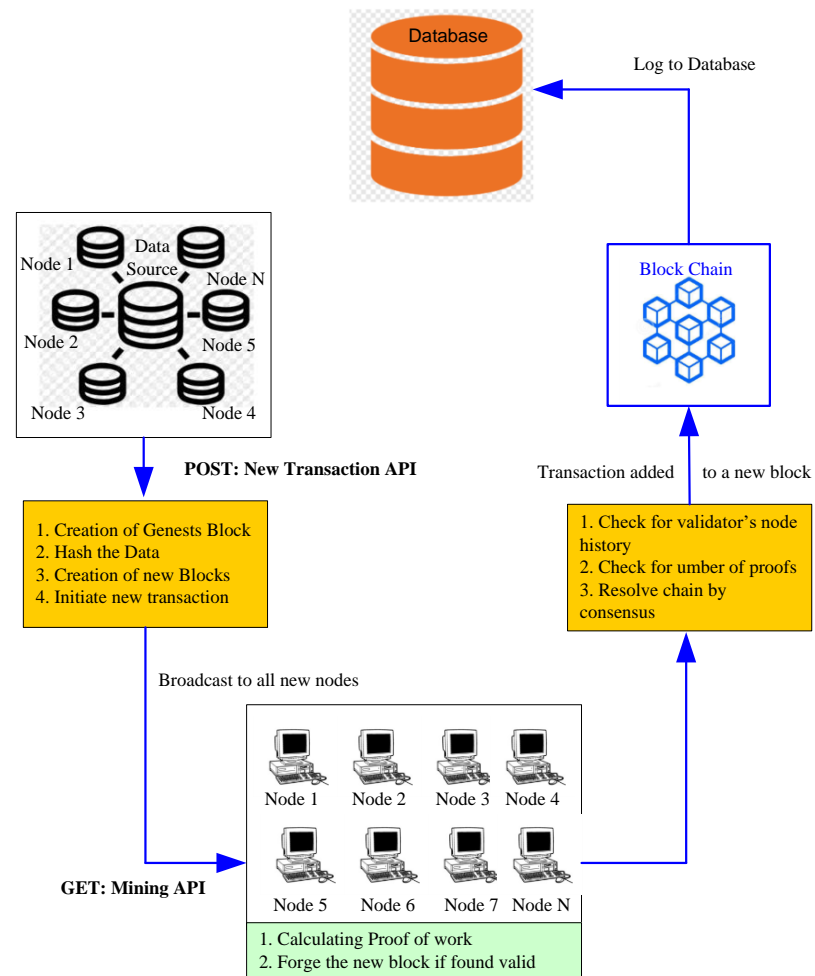


Figure 8. Process of blockchain connecting to the cloud server via API.

5. Hardware Implementation

The significance of the sensor node and blockchain-based Long-Range gateway configuration for real-time analysis of the nodes' filling state will be discussed in this section. Long-range modulation is used to establish the sensor node and gateway, where the gateway is incorporated with ESP 8266 Wi-Fi component for the transmission of data via Internet. As the sensor nodes are deployed in an outdoor location where the electrical grid network should not be used for powering the nodes because it increases the setup cost of installing an individual electric grid network, power consumption is initially the most important factor to consider when designing the nodes. We implanted the power connection for supplying power to the sensor node through batteries in the sensor node. The +5 V and +3.3 V voltage converters are integrated with the sensor node and gateway to provide the required voltage.

The range of a communication module plays an essential role in preventing the power dissipation in the nodes during the data transmission of the data. As a result, for Long-Range data transmission, a communication module with low power consumption is used. The control unit is another essential component to consider while designing the node. The control unit is chosen depending on the computing capacity needed to process the collected data, because the major goal of our study is to sense the filling data, the computational power required to analyze the obtained data is of minimal complexity in our study. To design an energy-efficient node, it is also important to choose the right microcontroller/microprocessor. Once the components for designing the nodes have been selected, now the next phase is to combine all these components on a single board for executing a flexible, reliable, and compatible node.

(a) Sensor Node:

The block diagram and prototype of the sensor node are shown in Figure 9. The Atmega 328P controller and SX 1278 Long-Range module transceiver are embedded in the node. PM sensor, CO sensor, ozone (O₃) sensor, and NO₂ sensor will be integrated to the sensor node for obtaining the sensor data of CO, PM_{2.5}, PM₁₀, NO₂, and ozone level in atmosphere. In this study, the complexity of the data which is being processed is very low, hence we chose the Atmega328P controller to compute the data because it uses the minimum amount of current(mA). In the sensor node, Tables 2 and 3 provide the technical specs of the Atmega328P microprocessor and the SX1278 Long-Range module.

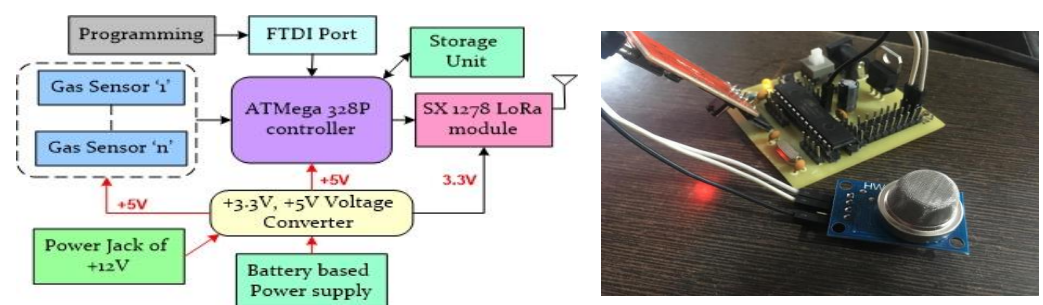


Figure 9. Sensor nodes.

Table 2. SX 1278 Long-Range specifications [31].

Characteristic	Specification
Network Topology	Point-to-Point, Point-to-Multipoint, Peer-to-Peer
Frequency	433 MHz
Modulation	FSK/GFSK/Long-Range/MSK
Data Rate	<300 kbps
Sensitivity	−136 dBm
Output Power	+20 dB
Operating Voltage	1.8 V to 3.6 V
RSSI	127 dB
Link budget	168 dB
Current	Tx: 120 mA, Rx: 10.8 mA

Table 3. ATmega328P specifications [32].

Characteristic	Specification
Architecture	RISC
Controller	8-bit microcontroller
Serial Interface	Master/slave SPI
Programming	In-system programming
Pin 6 analog pins	14 digital pins
PWM channels	6
Operating Voltage	2.7 V to 5.5 V
Current	Active state: 1.5 mA at 3 V–4 MHz, Power-down state: 1 μA at 3 V

(b) Long-Range-based Gateway:

The block diagram and prototype of the Long-Range -based gateway are shown in Figure 10. The gateway has an ATmega 328P controller, as well as an SX 1278 Long-Range transceiver, and an ESP 8266 Wi-Fi module. The focus of the gateway is to send data over several transmission protocols. The data are received by the SX 1278 Long-Range transceiver, and the ATmega 328P controller prompts the ESP 8266 Wi-Fi to send it through the Internet protocol. Table 4 shows the technical specifications of ESP 8266 Wi-Fi.

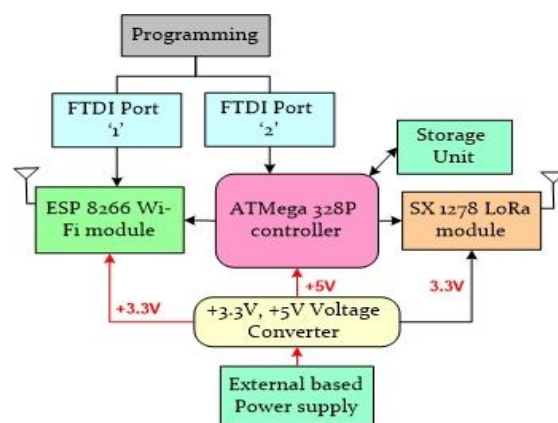


Figure 10. Long-Range-based gateway.

Table 4. Technical specifications of ESP 8266 [33].

Characteristic	Specification
Processor	Tensilica L106 32-bit processor
IEEE standard	802.11 b/g/n
Frequency	2.4 GHz
Data rate	72 Mbps
Network Protocols	IPv4, TCP/UDP, HTTP
Tx Power	20 dBm (802.11b) 17 dBm (802.11g) & 14 dBm (802.11n)
Rx Sensitivity	−91 dBm (802.11b), −75 dBm (802.11g) & −71 dBm (801.11n)
Operating Voltage	2.5 V to 3.6 V
Current	Average: 80 mA

6. Evaluation Metrics of LoRa Network

Spread-spectrum technology is used by the Long-Range communication protocol, which operates in unlicensed ISM bands (433 MHz in Asia, 868 MHz in Europe, and 915 MHz in North America) [34]. The resulting signal has low noisy levels, high check engaging adapt-ability, and is challenging to recognize [35]. Specific data on LPWAN innovation and the PHY layer are represented by many characteristics, including Bandwidth (BW), Code Rate (CR), Transmission power, and Spreading Factor (SF) in certain works that highlight Long-Range innovation. Furthermore, Long-Range base stations can receive messages con-currently that were delivered using certain spreading components [36]. LoRaWAN has multi-kilometer range, bi-directional availability, with data rates ranging from 0.3 kbps to 50 kbps. A frequency from one of three bands—125 kHz, 250 kHz, or 500 kHz—is shown in the spectrum band as BW. Smaller bandwidths are used for long-distance transmission, whereas larger bandwidths suggest speedier transmission. BW is the Long-Range modulation’s primary variable. The Long-Range symbol represents the whole frequency band, which is made up of 2SF chirps. It begins with a succession of ascending chirps; if the maximum frequency band is reached, the frequency is then covered, and it will grow once again from the lowest frequency. The speed at which bits are moved from one place to another is referred to as the bit rate or data rate. The bit rate (*Rbit*) of Long-Range is expressed as:

$$Rbit = \frac{SF * BW}{2^{SF} * BW} \quad (1)$$

The ability of a system to extract relevant information from signals is referred to as sensitivity. It can also be assessed as the weakest signal that can be received while still causing the system to packet resolution. The first term is produced by thermal noise in a bandwidth of 1 Hz and can only be controlled by adjusting the receiver’s temperature. The second term is denoted by the receiver bandwidth. The receiver’s noise figure (*NF*) is fixed for a specific hardware design. The signal-to-noise ratio required by the underlying modulation scheme is represented as *SNR*. The Long-Range designer has access to two design factors: bandwidth and signal-to-noise ratio (*SNR*). The Long-Range receiver sensitivity (*S*) is determined as follows:

$$S = -174 + 10 \log_{10} BW + NF + SNR \quad (2)$$

where *S* = receiver sensitivity in dB, *BW* = Bandwidth in kHz, *NF* = Noise Figure of a receiver in dB, and *SNR* = Signal-to-Noise Ratio. The behavior of the network is evaluated by varying certain parameters such as bandwidth, SF, and CR. The analysis of bit rate, and Long-Range sensitivity are presented below.

(a) Bit rate:

The number of bits sent between the transmitter and receiver during transmission is commonly referred to as the data rate or bit rate denoted by bits per second (bps). Equation (1) was used to determine the Long-Range bit rate. The equation includes input parameters such as SF, BW, and CR (1 to 4) to calculate the bit rate of Long-Range which is illustrated in Tables 5–8. The table demonstrate that SF is directly proportional to the BPS and when BW is increased the BPS is also increased. The bit rate of Long-Range from SF7 to SF12 is shown in Figure 11 for CR1 to CR4. The frequencies for BW1, BW2, and BW3 are 125 kHz, 250 kHz, and 500 kHz, respectively. It is concluded from the graphs that increase in CR and increase in bandwidth increase the bit rate.

Table 5. LoRa data rate/bit rate at CR1.

SF	LoRa Data Rate (BPS)		
	BW1 (125 kHz)	BW2 (250 kHz)	BW3 (500 kHz)
SF7	5468.75	10,937.5	21,875
SF8	3125	6250	12,500
SF9	1757.81	3515.62	7031.25
SF10	976.56	1953.12	3906.25
SF11	537.1	1074.21	2148.43
SF12	292.96	585.93	1171.87

Table 6. LoRa data rate/bit rate at CR2.

SF	LoRa Data Rate (BPS)		
	BW1 (125 kHz)	BW2 (250 kHz)	BW3 (500 kHz)
SF7	4557.29	9114.58	18,229.16
SF8	2604.16	5208.33	10,416.66
SF9	1464.84	2929.68	5859.37
SF10	813.8	1627.6	3255.2
SF11	447.59	895.18	1790.36
SF12	244.14	488.28	976.56

Table 7. LoRa data rate/bit rate at CR3.

SF	LoRa Data Rate (BPS)		
	BW1 (125 kHz)	BW2 (250 kHz)	BW3 (500 kHz)
SF7	3906.25	7812.5	15,625
SF8	2232.14	4464.28	8928.57
SF9	1255.58	2511.16	5022.32
SF10	697.54	1395.08	2790.17
SF11	383.64	767.29	1534.59
SF12	209.26	418.52	837.05

Table 8. LoRa data rate/bit rate at CR4.

SF	LoRa Data Rate (BPS)		
	BW1 (125 kHz)	BW2 (250 kHz)	BW3 (500 kHz)
SF7	3417.96	6835.93	13,671.87
SF8	1953.12	3906.25	7812.5
SF9	1098.63	2197.26	4394.53
SF10	610.35	1220.7	2441.4
SF11	335.69	671.38	1342.77
SF12	183.1	366.21	732.42

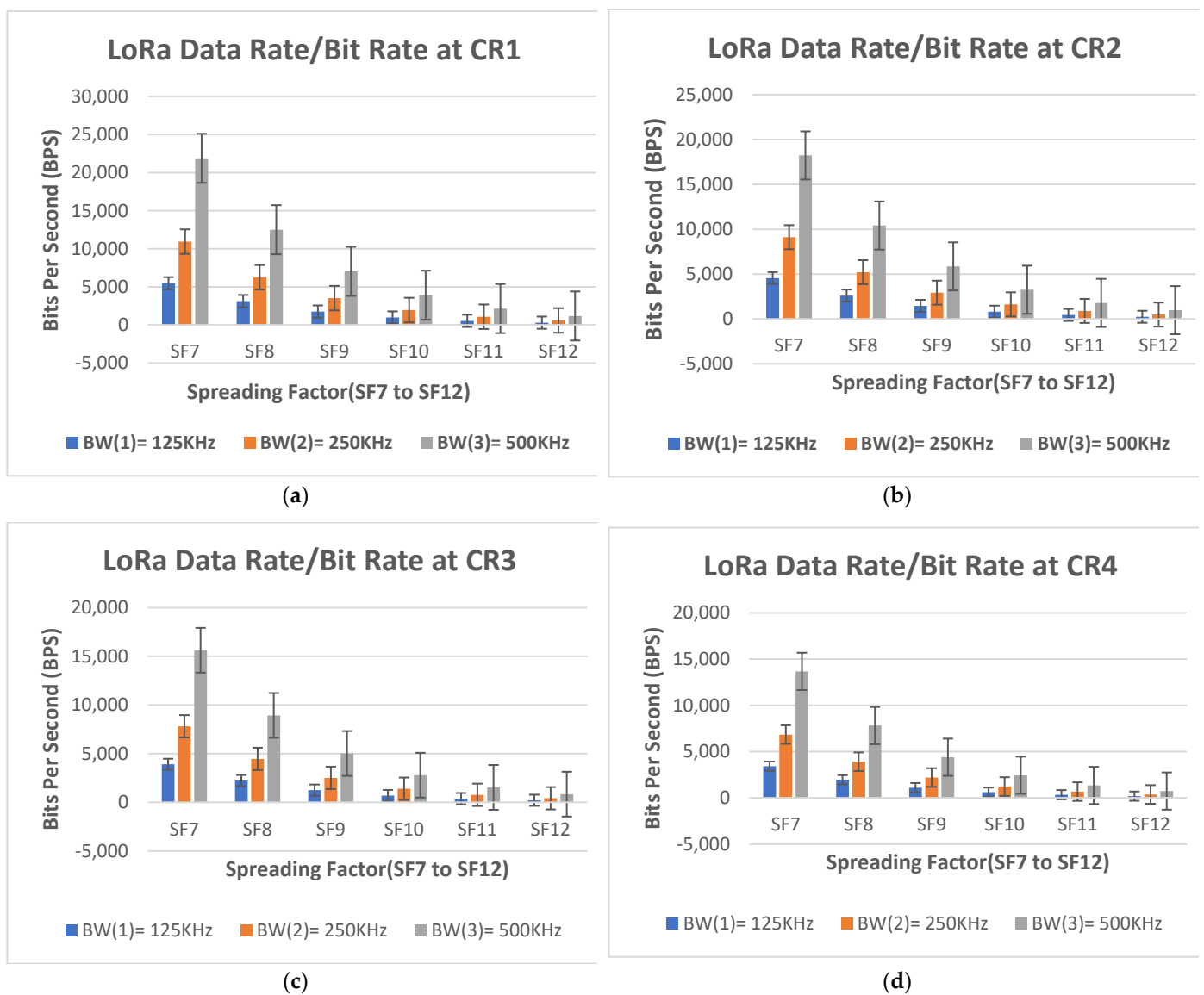


Figure 11. A bit rate of SF7-SF12 at CR1, CR2, CR3, CR4. (a) A bit rate of SF7-SF12 at CR1. (b) A bit rate of SF7-SF12 at CR2. (c) A bit rate of SF7-SF12 at CR3. (d) A bit rate of SF7-SF12 at CR4.

(b) Receiver sensitivity:

The input variables employed to determine the receiver’s long-range sensitivity are the BW, SF, and noise figure (NF). Equation (2) is used to obtain the results, and BW of 125 kHz, 250 kHz, and 500 kHz are also acknowledged. This BW is denoted by the following BW numbers: BW1 (125 kHz), BW2 (250 kHz), and BW3 (500 kHz) as shown in Table 9. For distinct SF, the signal-to-noise ratio (SNR) value varies. The SNR of -7.5 for SF7, -10 for SF8, -12.5 for SF9, -15 for SF10, 17.5 for SF11, and -20 for SF12 are considered. Normally, power sensitivity is expressed as a negative value, such as -127 dBm, and any value over that point denotes a decline in sensitivity. The sensitivity from the SF7 to the SF12 is shown in Figure 12; the SF7’s sensitivity power is highest at the BW10 (500 kHz), and the SF12’s sensitivity is lowest at the BW1 (7.8 kHz).

Table 9. Receiver sensitivity of LoRa.

SF	BW1	BW2	BW3	BW4	BW5	BW6	BW7	BW8	BW9	BW10
SF7	-150.07	-148.82	-147	-145	-144	-142	-141	-138	-135	-132
SF8	-155.07	-153.82	-152	-150	-149	-147	-146	-143	-140	-137
SF9	-160.07	-158.82	-157	-155	-154	-125	-151	-148	-145	-142
SF10	-165.07	-163.82	-162	-160	-159	-157	-156	-153	-150	-147
SF11	-170.07	-168.82	-167	-165	-164	-162	-161	-158	-155	-152
SF12	-175.07	-173.82	-172	-170	-169	-167	-166	-163	-160	-157

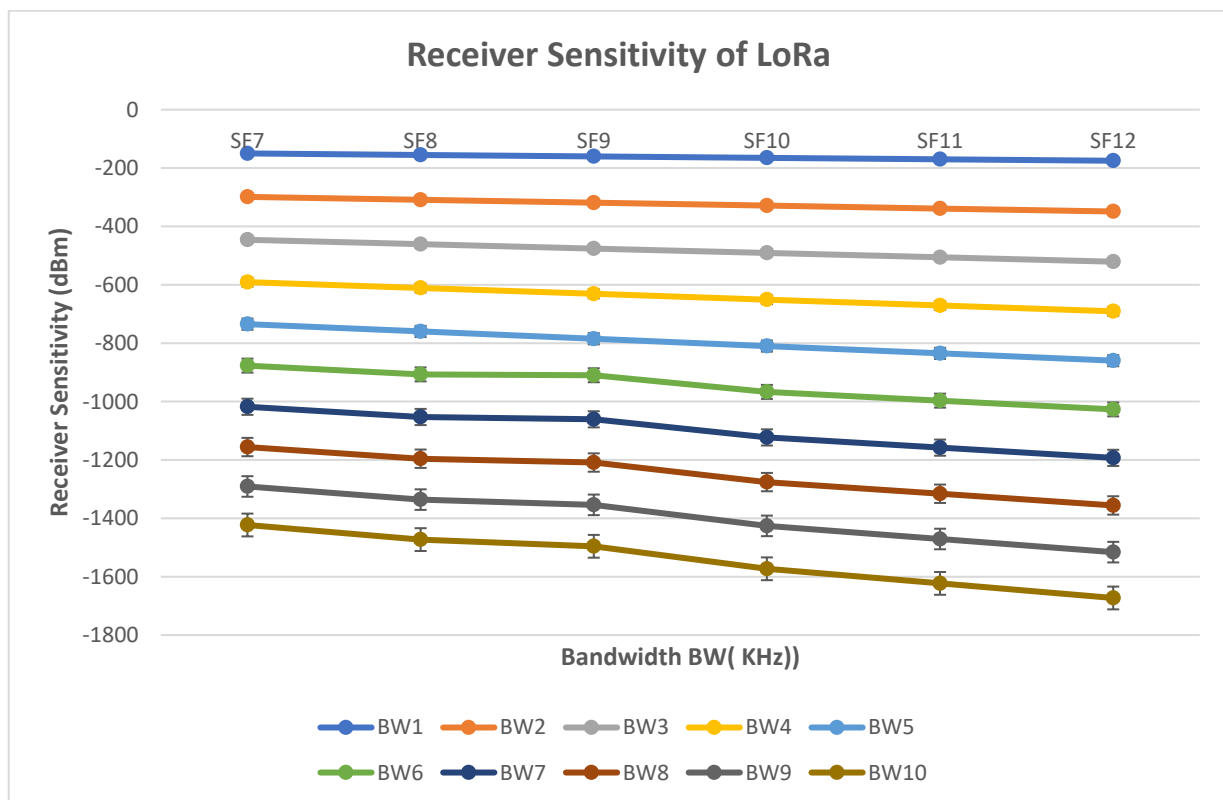


Figure 12. Receiver sensitivity of LoRa from SF7-SF12.

(c) Time on Air (ToA)

For calculating the ToA (ms), we used specific parameters such as preamble length in symbols = 8, payload length in bytes = 25, BW1 = 125 kHz, BW2 = 250 kHz, BW3 = 500 kHz, CF = 433 MHz. With the help of LoRa tool [37], the value for ToA is calculated from SF7 to SF12 at CR from 1 to 4 individually (Tables 10–13). Figure 13 depicts the ToA (ms) for the payload length of 25 bytes and preamble length of 8 symbols for different bandwidths from SF7 to SF12. Among all the three bandwidths, the ToA is high for the BW1 in SF12 and Low for the BW3 in SF7.

Table 10. Time on Air (ToA) (ms) at CR1.

SF	LoRa Data Rate (BPS)		
	BW1 (125 kHz)	BW2 (250 kHz)	BW3 (500 kHz)
SF7	56.58	28.29	14.14
SF8	102.91	51.46	25.73
SF9	205.82	102.91	51.46
SF10	370.69	185.34	92.67
SF11	741.38	370.69	185.34
SF12	1318.91	659.46	329.73

Table 11. Time on air (ToA) (ms) at CR2.

SF	LoRa Data Rate (BPS)		
	BW1 (125 kHz)	BW2 (250 kHz)	BW3 (500 kHz)
SF7	63.74	31.87	15.94
SF8	115.2	57.6	28.8
SF9	230.4	115.2	57.6
SF10	411.65	205.82	102.91
SF11	823.3	411.65	205.82
SF12	1449.98	724.99	362.5

Table 12. Time on air (ToA) (ms) at CR3.

SF	LoRa Data Rate (BPS)		
	BW1 (125 kHz)	BW2 (250 kHz)	BW3 (500 kHz)
SF7	70.91	35.46	17.73
SF8	127.49	63.74	31.87
SF9	254.98	127.49	63.74
SF10	425.61	226.3	113.15
SF11	905.22	452.61	226.3
SF12	1581.06	790.53	395.26

Table 13. Time on air (ToA) (ms) at CR4.

SF	LoRa Data Rate (BPS)		
	BW1 (125 kHz)	BW2 (250 kHz)	BW3 (500 kHz)
SF7	78.08	39.04	19.52
SF8	139.78	69.89	34.94
SF9	279.55	139.78	69.89
SF10	493.57	246.78	123.39
SF11	987.14	493.57	246.78
SF12	1712.13	856.06	428.03

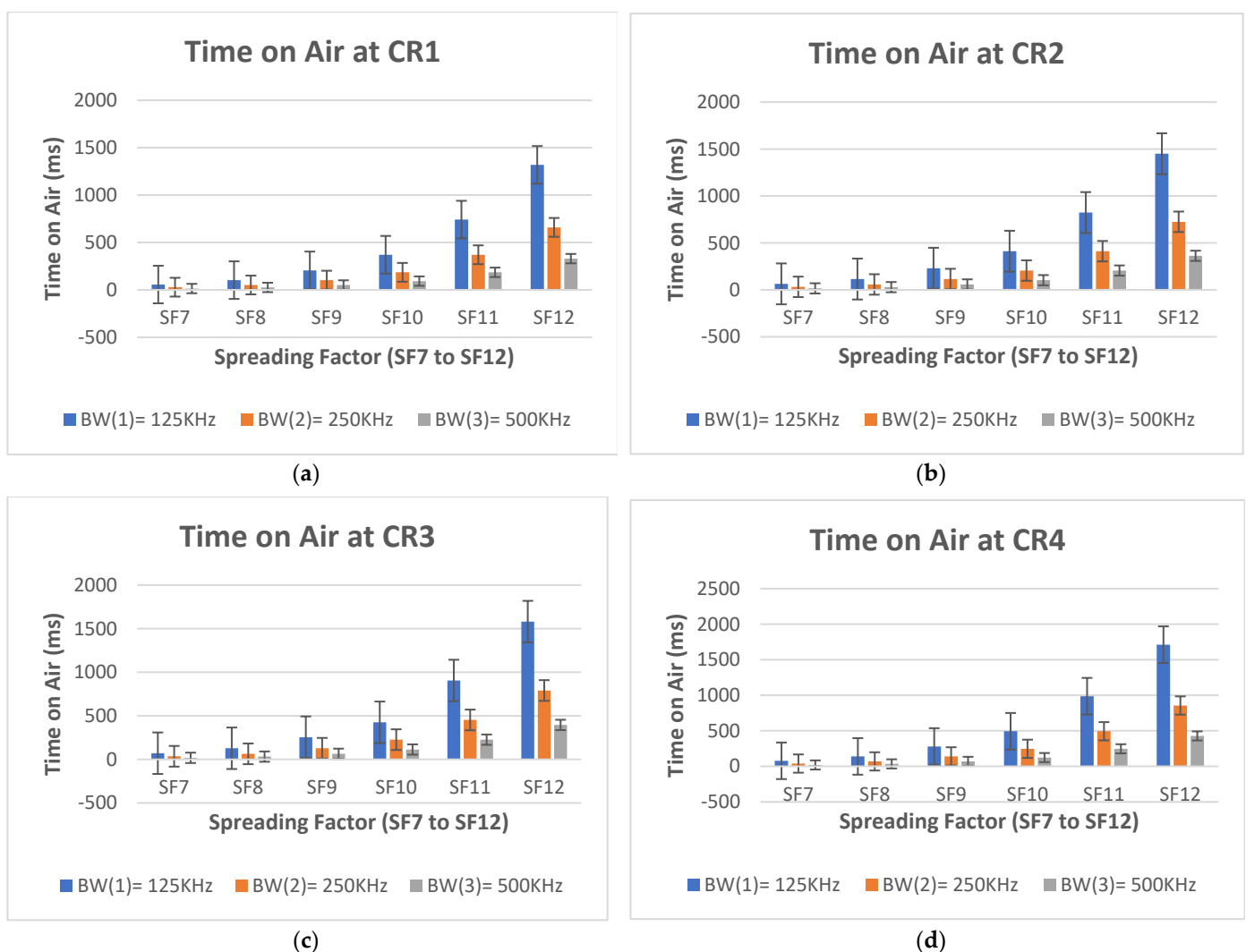


Figure 13. Time on air for a payload length of 25 bytes and preamble length of 8 symbols. (a) Time on air at CR1. (b) Time on air at CR2. (c) Time on air at CR3. (d) Time on air at CR4.

7. Results and Discussion

The proposed system is implemented in real-time in the location of Dehradun (Uttarakhand, India) with latitude: 30.3410° N, longitude: 77.9544° (Figure 4). A customized sensor mote based on 433 MHz frequency Long-Range is utilized for data transmission of sensors incorporated to it. The sensor mote is embedded with the ATmega 328 P controller, multiple power pins (+12 V, +5 V, +3.3 V). During firmware development of sensor

mote, it is programmed with multiple unique features such as node mapping, and symmetric encryption. Node mapping feature enables the sensor mote to minimize the data redundancy; symmetric encryption in the sensor mote enables to send the sensor data securely. During the implementation of LoRa network in hardware device for the moving vehicles, the receiver sensitivity concluded is -132 dBm (Spreading factor: 7; code rate: 4/8; transmit power: 2 dBm, bandwidth: 500 kHz). In the case of data rate, the data rate for the proposed study is 13,671.87 bits per second by considering the following parameters such as spreading factor: 7; code rate: 4/8; bandwidth: 500 kHz. As per the proposed architecture, the sensor mote is connected to the gateway through 433 MHz Long-Range module. In this study, we have integrated the PM sensor, CO sensor, ozone (O_3) sensor, and NO_2 sensor to monitor CO, $PM_{2.5}$, PM_{10} , NO_2 , and ozone level in atmosphere for the vehicle's pollution monitoring in the environment. A study has adopted these sensors for monitoring the vehicle emissions in the parking garages and with the motivation this study also adopted same sensors for monitoring the vehicle emissions [38]. CO sensor manufactured by Alphasense with range of 5–500 ppm is considered to monitor the CO level and it is analog sensor that is connected to the analog pin (A_0) of the sensor mote. PMS 5003 dust sensor is used to sense the $PM_{2.5}$, PM_{10} levels in the atmosphere. It is 8 pin sensor that comprises of V_{cc} (+5 V), GND, SET, R_{XD} , T_{XD} , RST, and two no connected pins. V_{CC} is connected to the +5 V of the sensor mote; R_{XD} , and T_{XD} pins are connected to the digital pins (D_0 , D_1), and GND is connected to ground of the sensor mote. MICS 2714 NO_2 sensor is able to sense the NO_2 level upto 0.05–10 ppm. It comprises of four pins such as V_0 , EN, GND and V_{cc} connected to the A_1 pin, D_2 pin, ground and +5 V of the sensor mote. MQ 131 Ozone sensor comprises four pins such as GND, analog out, digital out and V_{cc} and these pins are connected to ground, A_2 , D_3 pins of the sensor mote. These all sensors take below 3 min warm time to sense the value.

The calibration of the sensors is implemented in this study before implementation for error-free sensor values. We used a frequency agility-based interference avoidance algorithm in the gateway to detect interference and transfer it to a safe channel with minimal energy usage and latency while dealing with interference. Thingspeak server was employed in this study to visualize sensor value on the cloud server through an edge computing-based device and gateway. An API key of the thingspeak server loaded in the ESP 8266 Wi-Fi controller enables authentication and interfacing with hardware. As the sensor calibration and firmware development of the hardware is completed, the system is deployed in real-time as shown in Figure 4. Based on the deployment of the system, the sensor directs the sensing analog data to the ATmega 328P controller unit and the analog-to-digital converter converts the analog value into digital. The sensor values such as temperature, humidity level, and air pressure around the environment are processed in the sensor mote and transmitted to the gateway through an edge computing-based device through 433 MHz Long-Range module.

The different sensor values of the sensor mote are logged on the thingspeak server and they are visualized in Figures 14–16. Figure 14a of the thingspeak server dashboard visualizes the PM_{10} content of the location at two different time intervals. At 12:30 PM, the PM_{10} content recorded on the server is above 100 and when comparing this value in Table 14, the recorded PM_{10} is above the optimal range. This indicates that the PM_{10} content is high in the air and the health of the air needs to be moderate. Figure 14b of the thingspeak server dashboard visualizes the $PM_{2.5}$ content of the location at two different time intervals. At 12:30 PM, the $PM_{2.5}$ content recorded on the server is equal to 100 and when comparing this value in Table 14, the recorded $PM_{2.5}$ is above the optimal range. This indicates that the $PM_{2.5}$ content is high in the air and the health of the air is poor.

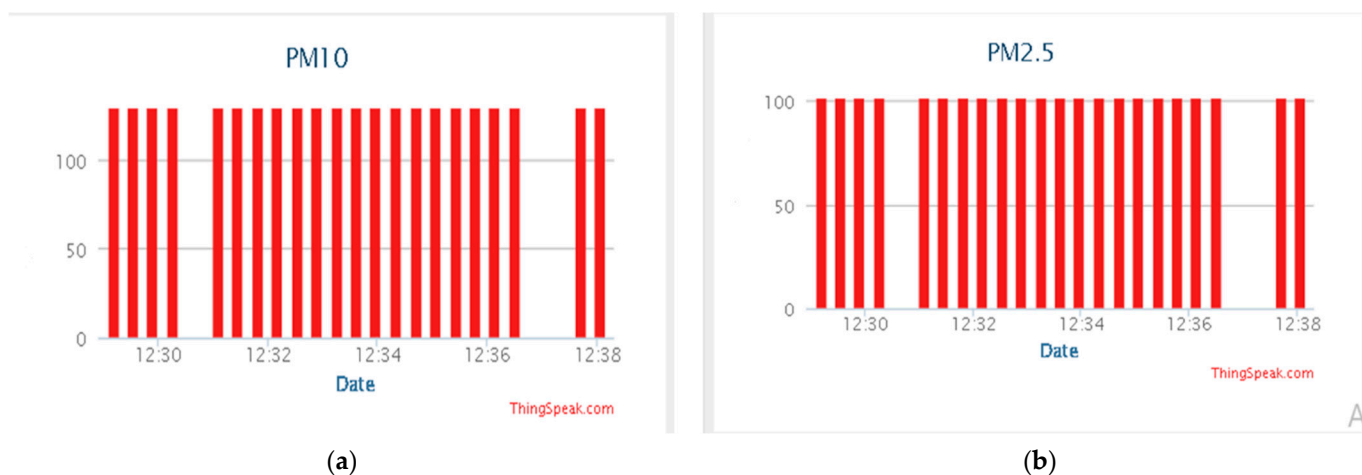


Figure 14. (a) PM₁₀ level (b) PM_{2.5} level.

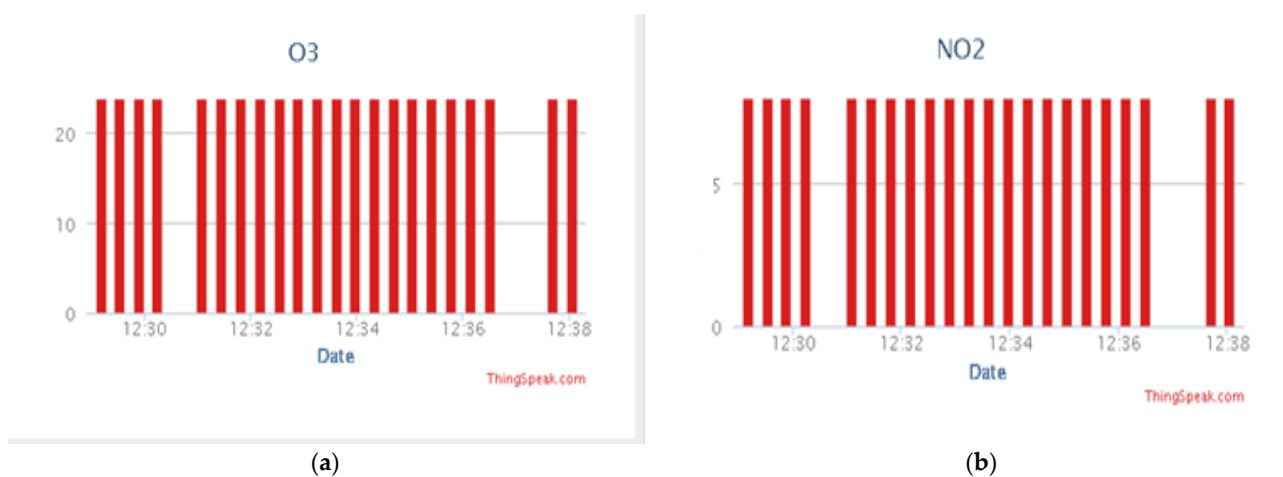


Figure 15. (a) O₃ level, (b) NO₂ level.

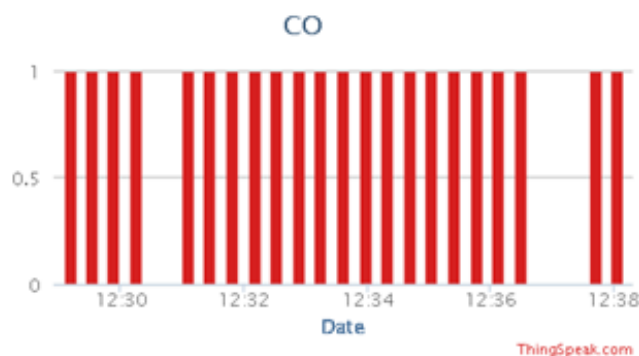


Figure 16. CO level.

Figure 15a of the thingspeak server dashboard visualizes the NO₂ content of the location at two different time intervals. At 12:30 PM, the NO₂ content recorded on the server is above 10 and when comparing this value in Table 14, the recorded NO₂ is in the optimal range. This indicates that the NO₂ content is normal in the air and the health of the air is good. Figure 15b of the thingspeak server dashboard visualizes the O₃ content of the location at two different time intervals. At 12:30 PM, the O₃ content recorded on the server is above 20 and when comparing this value in Table 14, the recorded O₃ is in the optimal range i.e., 0–50. This shows that the O₃ content is normal in the air and the health of the air is good.

Table 14. Air quality index computation table.

	Air Quality Index ($\mu\text{g}/\text{m}^3$) Category (Range)					
	Good (0–50)	Satisfactory (51–100)	Moderate (101–200)	Poor (201–300)	Very Poor (301–400)	Severe (401–500)
PM ₁₀ (24 h)	0–50	51–100	101–250	251–350	351–430	430 +
PM _{2.5} (24 h)	0–30	31–60	61–90	91–120	121–250	250 +
NO ₂ (24 h)	0–40	41–80	81–180	181–280	281–400	400 +
O ₃ (24 h)	0–50	51–100	101–168	169–208	209–748	748 + *
CO (24 h)	0–1.0	1.1–2.0	2.1–10	10.1–17	17.1–34	34 +

Note: + indicates if the numerical value exceeds the range, then the value is concludes that the air quality is severe.

* Indicates that the air quality is severe.

Figure 16 of the thingspeak server dashboard visualizes the CO content of the location at two different time intervals. At 12:30 PM, the CO content recorded on the server is equivalent to 1 and when comparing this value in Table 14, the recorded CO is in the optimal range i.e., 0–1.0. This indicates that the CO content is normal in the air and the health of the air is good.

Table 15 shows the comparison between previous literature surveys with proposed work. In [39], the performance of the device was verified and validated by measuring air quality by using PM sensor at several indoor and outdoor environments. In [40], a study shown that evaluates the precision, accuracy, and usefulness of a low-cost indoor air quality sensor in a domestic setting for collecting data on indoor pollution. Temperature, relative humidity, total VOC, CO₂ equivalents, and fine PM_{2.5} data were collected using five low-cost sensors and compared to data from other scientifically certified monitors. In [41], for industrial and urban regions, an outdoor WSN-based air quality monitoring system was proposed. A trio of gas sensors (O₃, CO, and NO₂), as well as a ZigBee wireless communication network based on Libelium's [42] gas sensing capable mote, make up the sensor node. The ZigBee is used to upload data to the central server. The public can get authorized air pollution information by email, SMS, and a tailored web app. In [43], it was only implemented for indoor air quality.

Table 15. Comparison of the previous literature survey with proposed work.

References	Parameters Considered	Communication	Customized Hardware	Gateway	Cloud Server	Blockchain Integration
[39]	PM	NA	Not Implemented	NA	No	No
[40]	Fine PM _{2.5} , CO ₂ , VOCs, RH, and temperature	Wi-Fi	Not Implemented	NA	Yes	No
[41]	O ₃ , CO, NO ₂	ZigBee + Wi-Fi	Not Implemented	Yes	Yes	No
[43]	CO, NO ₂ , O ₃ , CO ₂	ZigBee + Wi-Fi	Not Implemented	Yes	Yes	No
Proposed Work	PM ₁₀ , PM _{2.5} , NO ₂ , O ₃ , CO	Long-Range + Wi-Fi	Customized sensor node and gateway	Yes	Yes	Blockchain interfaced with hardware for node authentication

Each sensor node is made up of several sensors (temperature and relative humidity sensors, CO, methane, and solvent vapor sensors), as well as a Wi-Fi communication link. The proposed work tests the outdoor air quality with the help of sensor nodes PM₁₀, PM_{2.5}, NO₂, O₃, and CO which is set in vehicles. Long-Range gateway node is used to upload the data on the cloud server via Internet. The gateway converts RF transmissions into IP packets so that information can be communicated across the Internet protocol. In the previous studies, it has been identified that limited studies have implemented the customization

of hardware for the implementation of wireless-based system. To overcome transmission range and power consumption, this study has implemented long-range communication protocol with Internet of things network. Along with this, the blockchain integration with hardware is missing in the previous studies. In the proposed study any architecture is proposed to interface the blockchain network with hardware. In this study, low-cost sensors such as PM₁₀, PM_{2.5}, NO₂, O₃, and CO were used to collect the data and integrated cloud platform with blockchain system. Here blockchain ensure to collect sensor data by setting the threshold value for collecting and storing the data. The smart contracts assist to pre-trigger the alerts when it exceeds the threshold value.

8. Conclusions

Vehicle pollution monitoring using Internet of Things is required to monitor the air quality for a clean and healthy environment for the human beings. The implementation of Internet of Things system requires reliable and low power communication protocol for the transmission of real-time data. Blockchain technology plays an important role in today's scenario in terms of information security and transparency capabilities. In this study, we have proposed Long-Range and blockchain-based Internet of Things-inspired system with sensor node and gateway for real-time monitoring of vehicle pollution. Bit rate, receiver sensitivity, and time on air of the LoRa network are calculated by varying various parameters such as SF, CR, bandwidth, number of packets, payload size, preamble and noise figure. It is concluded from the evaluation that an increase in CR and increase in bandwidth increase the bit rate and, the ToA is high for the BW1 in SF12 and Low for the BW3 in SF7. The real-time implementation of the system is carried out by deploying the hardware and obtained real-time sensor values on the cloud server through Long-Range and Internet of Things connectivity. The sensor values recorded in the cloud server is compared with optimal values and concluded that the PM₁₀, PM_{2.5} are high in the air and remaining values of NO₂, O₃, CO are optimal in the air. Along with this an architecture is proposed for interfacing the hardware with blockchain network through cloud server and API for node authentication. As a part of future work and to overcome limitations, this study will carry out monitoring of individual vehicles emissions with low-cost sensors by mounting on vehicles with customized Internet of Things-based system.

Author Contributions: Conceptualization, A.R.; methodology, A.R. and A.A.; validation, S.V.A. and M.R.; formal analysis, A.G. and R.S.; writing—original draft preparation, A.R.; writing—review and editing, M.R. and A.A.; supervision, A.S.R. and S.S.A.; funding acquisition, A.A. All authors have read and agreed to the published version of the manuscript.

Funding: This study was funded by the Deanship of Scientific Research, Taif University Researchers Supporting Project number (TURSP-2020/148), Taif University, Taif, Saudi Arabia.

Institutional Review Board Statement: Not applicable.

Informed Consent Statement: Not applicable.

Data Availability Statement: Data in this research paper will be shared on request to the corresponding author.

Acknowledgments: The authors would like to thank the Deanship of Scientific Research, Taif University Researchers Supporting Project number (TURSP-2020/148), Taif University, Taif, Saudi Arabia for supporting this research work.

Conflicts of Interest: The authors declare no conflict of interest.

References

1. Gubbi, J.; Buyya, R.; Marusic, S.; Palaniswami, M. Internet of things (Internet of Things): A vision, architectural elements, and future directions. *Future Gener. Comp. Syst.* **2013**, *29*, 1645–1660. [[CrossRef](#)]
2. Xu, L.D.; He, W.; Li, S. Internet of things in industries: A survey. *IEEE Trans. Ind. Inform.* **2014**, *10*, 2233–2243. [[CrossRef](#)]
3. Balamurugan, S.; Saravanakamalam, D. Energy monitoring and management using internet of things. In Proceedings of the International Conference on Power and Embedded Drive Control (ICPEDC), Chennai, India, 16–18 March 2017; pp. 208–212.

4. Mohod, S.W.; Deshmukh, R.S. Internet of Things for Industrial Monitoring and Control Applications. *Int. J. Sci. Eng. Res.* **2016**, *7*, 494–498.
5. Rawat, A.S.; Rajendran, J.; Ramiah, H.; Rana, A. Long-Range (Long Range) and Long-Range WAN Technology for Internet of Things Applications in COVID-19 Pandemic. In Proceedings of the International Conference on Advances in Computing, Communication & Materials (ICACCM), Dehradun, India, 21–22 August 2020; pp. 419–422.
6. Reşitoğlu, İ.A.; Altinişik, K.; Keskin, A. The pollutant emissions from diesel-engine vehicles and exhaust aftertreatment systems. *Clean Technol. Environ. Policy* **2015**, *17*, 15–27. [[CrossRef](#)]
7. Manisalidis, I.; Stavropoulou, E.; Stavropoulos, A.; Bezirtzoglou, E. Environmental and Health Impacts of Air Pollution: A Review. *Front. Public Health* **2020**, *8*, 14. Available online: <https://www.frontiersin.org/article/10.3389/fpubh.2020.00014> (accessed on 15 June 2022). [[CrossRef](#)] [[PubMed](#)]
8. Kumar, P.G.; Lekhana, P.; Tejaswi, M.; Chandrakala, S. Effects of vehicular emissions on the urban environment—a state of the art. *Mater. Today Proc.* **2021**, *45*, 6314–6320. [[CrossRef](#)]
9. Available online: <https://www.nps.gov/subjects/air/sources.htm> (accessed on 15 June 2022).
10. Zanella, A.; Bui, N.; Castellani, A.; Vangelista, L.; Zorzi, M. Internet of things for smart cities. *IEEE Internet Things J.* **2014**, *1*, 22–32. [[CrossRef](#)]
11. Monzon, A. Smart cities concept and challenges: Bases for the assessment of smart city projects. In Proceedings of the International Conference on Smart Cities and Green ICT Systems, Prague, Czech Republic, 2–4 May 2015; pp. 1–11.
12. Sayed, E.; Ahmed, A.; Yousef, M.E. Internet of things in Smart Environment: Concept, Applications, Challenges, and Future Directions. *World Sci. News* **2019**, *134*, 1–51.
13. Jovanovska, E.M.; Davcev, D. No pollution Smart City Sightseeing Based on WSN Monitoring System. In Proceedings of the 2020 Sixth International Conference on Mobile And Secure Services (MobiSecServ), Miami Beach, FL, USA, 22–23 February 2020; pp. 1–6.
14. Pathak, A.; Uddin, M.A.; Jainal Abedin, M.; Andersson, K.; Mustafa, R.; Hossain, M.S. Internet of Things based smart system to support agricultural parameters: A case study. *Procedia Comput. Sci.* **2019**, *155*, 648–653. [[CrossRef](#)]
15. Reshi, A.A.; Shafi, S.; Kumaravel, A. VehNode: Wireless Sensor Network platform for automobile pollution control. In Proceedings of the 2013 IEEE Conference on Information & Communication Technologies, Thuckalay, India, 11–12 April 2013; pp. 963–966. [[CrossRef](#)]
16. Prasanth, L.; Sreekanthan, D.; Lakshmi, D.A.; Harikumar, G.; Vissutha, M.P.; Anjali, T. Intelligent Traffic Control System Using WSN: A Perspective. In Proceedings of the 2021 Fourth International Conference on Microelectronics, Signals & Systems (ICMSS), Kollam, India, 18–19 November 2021; pp. 1–5. [[CrossRef](#)]
17. Salman, N.; Kemp, A.H.; Khan, A.; Noakes, C.J. Real Time Wireless Sensor Network (WSN) based Indoor Air Quality Monitoring System. *IFAC-PapersOnLine* **2019**, *52*, 324–327, ISSN 2405-8963. [[CrossRef](#)]
18. Yi, W.Y.; Lo, K.M.; Mak, T.; Leung, K.S.; Leung, Y.; Meng, M.L. A Survey of Wireless Sensor Network Based Air Pollution Monitoring Systems. *Sensors* **2015**, *15*, 31392–31427. [[CrossRef](#)] [[PubMed](#)]
19. Hu, Z.; Tang, H. Design and Implementation of Intelligent Vehicle Control System Based on Internet of Things and Intelligent Transportation. *Sci. Program.* **2022**, *2022*, 6201367. [[CrossRef](#)]
20. Makhija, J.; Nakkeeran, M.; Anantha Narayanan, V. Detection of Vehicle Emissions Through Green Internet of Things for Pollution Control. In *Advances in Automation, Signal Processing, Instrumentation, and Control. Lecture Notes in Electrical Engineering*; Komanapalli, V.L.N., Sivakumaran, N., Hampannavar, S., Eds.; Springer: Singapore, 2021; Volume 700. [[CrossRef](#)]
21. Sharma, R.; Arya, R. UAV-based long-range environment monitoring system with Industry 5.0 perspectives for smart city infrastructure. *Comput. Ind. Eng.* **2022**, *168*, 108066, ISSN 0360-8352. [[CrossRef](#)]
22. Zheng, K.; Zhao, S.; Yag, Z.; Xiong, X.; Xiang, W. Design and implementation of LPWAbased air quality monitoring system. *IEEE Access* **2016**, *4*, 3238–3245. [[CrossRef](#)]
23. Balasubramaniyan, C.; Manivannan, D. Internet of Things enabled air quality monitoring system (AQMS) using Raspberry Pi. *Indian J. Sci. Technol.* **2016**, *9*, 1–6. [[CrossRef](#)]
24. Sofia, D.; Lotrecchiano, N.; Trucillo, P.; Giuliano, A.; Terrone, L. Novel Air Pollution Measurement System Based on Ethereum Blockchain. *J. Sens. Actuator Netw.* **2020**, *9*, 49. [[CrossRef](#)]
25. Dhingra, S.; Madda, R.B.; Gandomi, A.H.; Patan, R.; Daneshmand, M. Internet of Things Mobile–Air Pollution Monitoring System (Internet of Things–Mobair). *IEEE Internet Things J.* **2019**, *6*, 5577–5584. [[CrossRef](#)]
26. Camarillo-Escobedo, R.; Flores, J.L.; Marin-Montoya, P.; García-Torales, G.; Camarillo-Escobedo, J.M. Smart Multi-Sensor System for Remote Air Quality Monitoring Using Unmanned Aerial Vehicle and Long-Range WAN. *Sensors* **2022**, *22*, 1706. [[CrossRef](#)] [[PubMed](#)]
27. Yeh, W.C.; Lin, J.S. New parallel swarm algorithm for smart sensor systems redundancy allocation problems in the Internet of Things. *J. Supercomput.* **2018**, *74*, 4358–4384. [[CrossRef](#)]
28. Zhang, R.; Xue, R.; Liu, L. Security and privacy on blockchain. *ACM Comput. Surv.* **2019**, *52*, 1–34. [[CrossRef](#)]
29. Khan, S.N.; Loukil, F.; Ghedira-Guegan, C.; Benkhelifa, E.; Bani-Hani, A. Blockchain smart contracts: Applications, challenges, and future trends. *Peer-Peer Netw. Appl.* **2021**, *14*, 2901–2925. [[CrossRef](#)] [[PubMed](#)]
30. Wang, S.; Ouyang, L.; Yuan, Y.; Ni, X.; Han, X.; Wang, F.Y. Blockchain-enabled smart contracts: Architecture, applications, and future trends. *IEEE Trans. Syst. Man Cybern. Syst.* **2019**, *49*, 2266–2277. [[CrossRef](#)]

31. Lo Re, G.; Peri, D.; Vassallo, S. Urban Air Quality Monitoring Using Vehicular Sensor Networks. In *Advances onto the Internet of Things*; Gaglio, S., Lo Re, G., Eds.; Springer International Publishing: Gewerbestrasse, Switzerland, 2014; pp. 311–323.
32. Semtech Corporation. SX1276/77/78/79—137 MHz to 1020 MHz Low Power Long Range Transceiver. 2016. Available online: <https://www.scribd.com/document/399165229/SX1276-1278> (accessed on 15 June 2022).
33. Atmel Corporation. Data Sheet ATmega328P. 2015, pp. 1–294. Available online: http://ww1.microchip.com/downloads/en/DeviceDoc/Atmel-7810-Automotive-Microcontrollers-ATmega328P_Datasheet.pdf (accessed on 15 June 2022).
34. Ray, P.P. A survey of IoT cloud platforms. *Futur. Comput. Inform. J.* **2016**, *1*, 35–46. [CrossRef]
35. Pipeline Incident 20 Year Trends—PHMSA. Available online: <https://www.phmsa.dot.gov/data-and-statistics/pipeline/pipeline-incident-20-year-trends> (accessed on 12 July 2022).
36. Sendra, S.; García, L.; Lloret, J.; Bosch, I.; Vega-Rodríguez, R. Long-RangeWAN network for fire monitoring in rural environments. *Electronics* **2020**, *9*, 531. [CrossRef]
37. LoRaTool. Available online: <https://www.loratools.nl> (accessed on 13 July 2022).
38. Liu, B.; Zimmerman, N. Fleet-based vehicle emission factors using low-cost sensors: Case study in parking garages. *Transp. Res. Part D Transp. Environ.* **2021**, *91*, 102635, ISSN 1361-9209. [CrossRef]
39. Surannavar, K.; Tatwanagi, M.b.; Nadaf, S.P.; Hunshal, P.B.; Patil, D. Vehicular pollution monitoring system and detection of vehicles causing global warming. *Int. J. Eng. Sci. Comput.* **2017**, *7*, 12611–12614. [CrossRef]
40. Wu, Y.C.; Shiledar, A.; Li, Y.C.; Wong, J.; Feng, S.; Chen, X.; Chen, C.; Jin, K.; Janamian, S.; Yang, Z.; et al. Air quality monitoring using mobile microscopy and machine learning. *Light Sci. Appl.* **2017**, *6*, e17046. [CrossRef]
41. Moreno-Rangel, A.; Sharpe, T.; Musau, F.; McGill, G. Field evaluation of a low-cost indoor air quality monitor to quantify exposure to pollutants in residential environments. *J. Sens. Sens. Syst.* **2018**, *7*, 373–388. [CrossRef]
42. Libelium Libelium Waspote. Available online: <http://www.libelium.com/products/waspote/> (accessed on 27 May 2015).
43. Mansour, S.; Nasser, N.; Karim, L.; Ali, A. Wireless Sensor Network-based air quality monitoring system. In Proceedings of the 2014 International Conference on Computing, Networking and Communications (ICNC), Honolulu, HI, USA, 3–6 February 2014; pp. 545–550.